Journal of Power Sources 183 (2008) 506–511

Contents lists available at ScienceDirect

Journal of Power Sources

journal homepage: www.elsevier.com/locate/jpowsour

Electrochemical characteristics of an $La_{0.6}Sr_{0.4}Co_{0.2}Fe_{0.8}O_3$–$La_{0.8}Sr_{0.2}MnO_3$ multi-layer composite cathode for intermediate-temperature solid oxide fuel cells

Chao Jin, Jiang Liu*, Weimin Guo, Yaohui Zhang

School of Chemistry and Chemical Engineering, South China University of Technology, 381 Wushan Road, Guangzhou 510641, PR China

ARTICLE INFO

Article history:
Received 31 March 2008
Received in revised form 16 May 2008
Accepted 20 May 2008
Available online 27 May 2008

Keywords:
Solid oxide fuel cell
LSCF
LSM
Multi-layer composite cathode
Cathodic polarization

ABSTRACT

An $La_{0.6}Sr_{0.4}Co_{0.2}Fe_{0.8}O_3$–$La_{0.8}Sr_{0.2}MnO_3$ (LSCF–LSM) multi-layer composite cathode for solid oxide fuel cells (SOFCs) was prepared on an yttria-stabilized zirconia (YSZ) electrolyte by the screen-printing technique. Its cathodic polarization curves and electrochemical impedance spectra were measured and the results were compared with those for a conventional LSM/LSM–YSZ cathode. While the LSCF–LSM multi-layer composite cathode exhibited a cathodic overpotential lower than 0.13 V at 750 °C at a current density of 0.4 A cm^{-2}, the overpotential for the conventional LSM–YSZ cathode was about 0.2 V. The electrochemical impedance spectra revealed a better electrochemical performance of the LSCF–LSM multi-layer composite cathode than that of the conventional LSM/LSM–YSZ cathode; e.g., the polarization resistance value of the multi-layer composite cathode was 0.25 Ω cm^2 at 800 °C, nearly 40% lower than that of LSM/LSM–YSZ at the same temperature. In addition, an encouraging output power from an YSZ-supported cell using an LSCF–LSM multi-layer composite cathode was obtained.

1. Introduction

Nowadays, of the many possible sorts of perovskite-type material for solid oxide fuel cells (SOFCs), strontium-doped lanthanum manganite (LSM) is one of the most commonly used cathode materials. It is a good electronic conductor, with a conductivity range of 200–300 S cm^{-1} at 900 °C. It is stable up to 1200 °C with the widely used electrolyte material, 8 mol% yttria-stabilized zirconia (YSZ) [1–4], and its electrochemical activity for oxygen reduction is high at higher temperatures (800–1000 °C) [3,5]. However, the oxygen-ion conductivity of LSM is very low (10^{-7} S cm^{-1} at 900 °C and even lower at reduced temperatures [6]), and its activation energy for oxygen dissociation is high [7], which seriously limit the use of LSM cathodes in the development of intermediate-temperature SOFCs (operating at 600–800 °C). Much work has been devoted to the LSM material, and its properties as the cathode of an YSZ-electrolyte SOFC are well characterized. For example, Tsai and Barnett found that adding some YSZ electrolyte to the LSM to form a LSM–YSZ composite cathode dramatically improved the electrochemical performance of the cathode [4]. This phenomenon is attributed to the extension of the three-phase boundary (TPB) of the electrolyte (ionic conductor), cathode (electronic conductor), and gas phase (oxygen or air used as an oxidant). A good adhesion of the LSM–YSZ composite cathode layer to the YSZ electrolyte substrate can be easily realized by co-firing, because good connections will be established through the YSZ existing in both the cathode and the electrolyte. Similarly to LSM, $La_{0.6}Sr_{0.4}Co_{0.2}Fe_{0.8}O_3$ (LSCF) is a good electronic conductor. Some lectures reported that the conductivity of LSCF was larger than 300 S cm^{-1} at 600–800 °C [8,9]. At the same time, it has a very high oxygen diffusion coefficient and its oxygen-ion conductivity is 0.2 S cm^{-1} at 900 °C [10,11]. The high oxygen-ion conductivity makes LSCF the most promising candidate for intermediate-temperature SOFCs. Unfortunately, it reacts with YSZ to form $SrZrO_3$ and/or $La_2Zr_2O_7$ insulating phase(s) at temperatures as low as 800 °C [12]. It also has a larger thermal-expansion coefficient (TEC) than YSZ [13]. Therefore, an LSCF electrode is usually used with a doped ceria electrolyte, such as GDC (gadolinium-doped ceria) or SDC (samarium-doped ceria) at low temperatures.

To get the benefits of both LSM and LSCF for an YSZ-electrolyte SOFC, we have prepared a multi-layer composite cathode made of LSCF and LSM on an YSZ electrolyte substrate using the screen-printing technique. The configuration and components of the cathode are shown schematically in Fig. 1. In order to get a better adhesion to the YSZ electrolyte substrate, the LSM–YSZ composite cathode is applied as the first layer, and the LSM–SDC composite cathode is printed as the second layer to extend the zone of the TPB. SDC is used here instead of YSZ because it has a larger ionic

* Corresponding author. Tel.: +86 20 22236168; fax: +86 20 22236168.
E-mail address: jiangliu@scut.edu.cn (J. Liu).

0378-7753/$ – see front matter © 2008 Elsevier B.V. All rights reserved.
doi:10.1016/j.jpowsour.2008.05.049

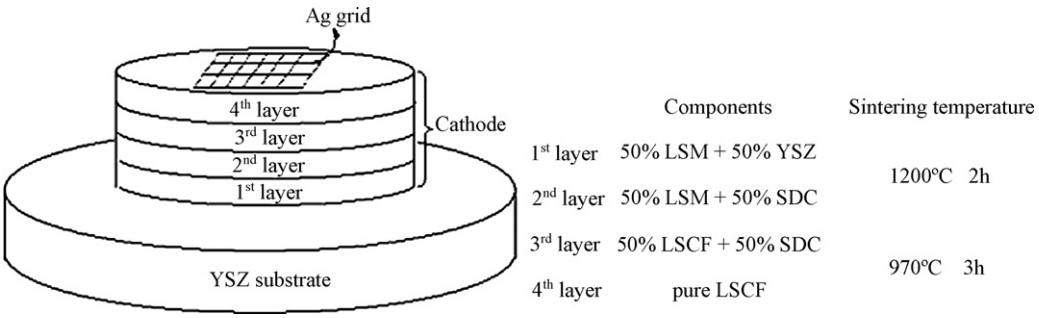

Fig. 1. Schematic diagram and components of the four-layer cathode half-cell structure.

conductivity and can also prevent the formation of $SrZrO_3$ and/or $La_2Zr_2O_7$ insulating phase(s) between YSZ and LSCF, which appears in the third layer with SDC. Finally, a pure LSCF-layer is printed on the top of the cathode to collect current effectively, as the electronic conductivity of pure LSCF is the highest among all the components in the multi-layer cathode. This novel multi-layer LSCF–LSM composite cathode was compared with the conventional LSM/LSM–YSZ cathode through electrochemical performance measurements.

2. Experimental

LSM and LSCF powders were prepared by a combined citric acid and ethylenediamine tetraacetic acid (EDTA) complexing method [14,15]. First, ($La(NO_3)_3{\cdot}6H_2O$, $Sr(NO_3)_2$, $Mn(NO_3)_2$, $Co(NO_3)_3{\cdot}6H_2O$ and $Fe(NO_3)_3{\cdot}9H_2O$) were mixed according to the stoichiometric compositions of LSM and LSCF, respectively, and dissolved in water; then the nitrate solution was mixed with a previously prepared 1 M EDTA–NH_4OH solution. After that, a certain amount of citric acid was introduced, and the mole ratio of the total metal ion:EDTA acid:citric acid was controlled around 1:1:1.5. NH_4OH was added to adjust the pH value to about 6.0. A brown gel was obtained after the solution was agitated for 12 h at 80 °C. This gel was held at 200 °C for several hours to remove organics and form a powder precursor. Finally, the LSM powder precursor was calcined at 1000 °C for 4 h and the LSCF precursor was calcined at 950 °C for 6 h. The $Ce_{0.8}Sm_{0.2}O_{1.9}$ (SDC) powders were prepared according to Ref. [16]. The crystal structure of the powders was examined with X-ray diffraction (XRD) using a Bede D1 X-ray diffractometer (UK, Bede Scientific Ltd.; Cu Kα radiation; operated at 40 kV, 45 mA; λ = 0.15418 nm), the diffraction angle ranging from 20° to 80° with a step of 0.02° and a rate of 1.2° min^{-1}.

The YSZ electrolyte substrates were made by pressing YSZ powders into pellets with a stainless-steel dye (13 mm in diameter) under a pressure of about 300 MPa. The pellets were sintered at 1400 °C in air for 4 h. The thickness of the sintered pellets was about 0.5 mm. As shown in Fig. 1, the multi-layer composite cathode was prepared by screen-printing several layers of different materials on the YSZ substrate in sequence. The first layer was LSM–YSZ and the second layer was LSM–SDC (50:50 weight ratio). They were co-sintered at 1200 °C for 2 h before the next layer was printed. The next layer was LSCF–SDC (50:50 weight ratio), followed by a layer of pure LSCF. Then, the pellet was sintered at 970 °C for 3 h. A conventional LSM/LSM–YSZ cathode was prepared in a similar way. Five layers of LSM–YSZ (50:50 weight ratio) were first printed on the YSZ substrate, and then one layer of pure LSM was prepared. Finally, they were co-sintered at 1200 °C for 2 h.

The interfacial polarization resistance (R_p) values of four different cells (shown in Table 1) were determined on symmetric cells with a two-electrode configuration in air. The overpotential was measured on the cells with a three-electrode method. A regular Ag counter electrode was applied symmetrically opposite to the cathode. An Ag point reference electrode was attached on the free YSZ surface, 3 mm away from the cathode [7,17,18]. The area of the cathode was 0.20 cm^2. The current collector was made by printing an Ag grid on the cathode, the grid covering the whole surface of the cathode. The width of the silver lines constituting the grid was about 0.05 mm, and the distance between two adjacent lines was about 0.20 mm. Before testing, the half-cell was heated at 200 °C for 2 h.

An YSZ electrolyte-supported SOFC was also prepared and tested using the two-electrode method. NiO and YSZ powders were first mixed at a weight ratio of 50:50. This mixture was then combined with an organic binder (ethyl cellulose, α-terpineol) in a weight ratio of 1:1 to form an anode paste. This paste was painted on one side of the YSZ substrate and sintered at 1400 °C for 4 h. After that, the multi-layer composite cathode layers were screen printed in turn on the other side of YSZ substrate and sintered. Silver paste was used to seal the SOFC and silver wire as the conductor leading the current out [19,20]. During electrochemical measurement of the SOFC, the cathode was exposed to ambient air, while the anode was exposed to fuel (pure hydrogen humidified with 3 vol.% water at 25 °C). The flow rate of the fuel was 50 sccm min^{-1}.

Electrochemical impedance spectroscopy (EIS), overpotential measurement of the half-cells and the performance measurements of the YSZ electrolyte-supported SOFC were carried out with an OUTLAB-PGSTAT30 electrochemical analyzer. For EIS measurement, the frequency ranged from 0.1 to 100 kHz and the AC amplitude was 5 mV. For overpotential measurement of the half-cell, IR was compensated. After testing, scanning electron microscopy (SEM) was used to observe the microstructure of the cells.

3. Results and discussion

3.1. Chemical stability of the cathode material

Fig. 2(a) and (c) is the XRD patterns of the LSM and LSCF final powders, respectively, synthesized through a combined citric acid and EDTA complexing method. It was observed that LSM and LSCF crystallized in a single phase with perovskite structure, and no

Table 1
Components and fabrication process of the four symmetrical cells

Cathodic components	Printed times			
	Cell a	Cell b	Cell c	Cell d
1st layer: 50%LSM–50%YSZ	1	1	1	5
2nd layer: 50%LSM–50%SDC	1	2	3	0
3rd layer: 50%LSCF–50%SDC	3	2	1	0
4th layer: pure LSCF	1	1	1	0
4th layer: pure LSM	0	0	0	1

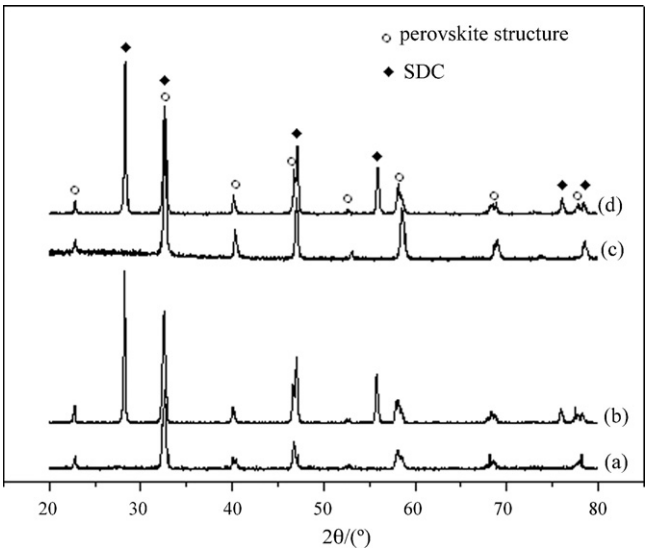

Fig. 2. XRD patterns of (a) LSM final powder; (b) LSM–SDC mixture sintered at 1200 °C for 2 h; (c) LSCF final powder; (d) LSCF–SDC mixture sintered at 970 °C for 3 h.

impurities were found [8,15]. As we know, the reaction of LSCF, LSM, and SDC with each other is undesirable for the long-term stability of SOFCs. The reactivity of LSM and LSCF with SDC was further studied. Fig. 2(b) shows the XRD pattern of the LSM–SDC mixture prepared by thoroughly mixing LSM with SDC powders in a 1:1 weight ratio, and then sintering at 1200 °C for 2 h. Fig. 2(d) is the XRD pattern of the LSCF–SDC mixture prepared by thoroughly mixing LSCF with SDC powders in a 1:1 weight ratio, and then sintering at 970 °C for 3 h. Clearly, there were no new peaks identifiable and no shift of XRD peaks in Fig. 2(b) and (d), indicating that there are no reaction and/or inter-diffusion of elements occurred within the composite cathode.

3.2. Impedance spectra of symmetric cathode cell

Fig. 3 shows the impedance spectra of the symmetric cathode cell for four cells obtained at 800 °C in air. The interfacial polarization resistances decreased when the LSCF–LSM multi-layer composite cathode was used. Moreover, compared with the cathode components and the interfacial polarization resistances of cells

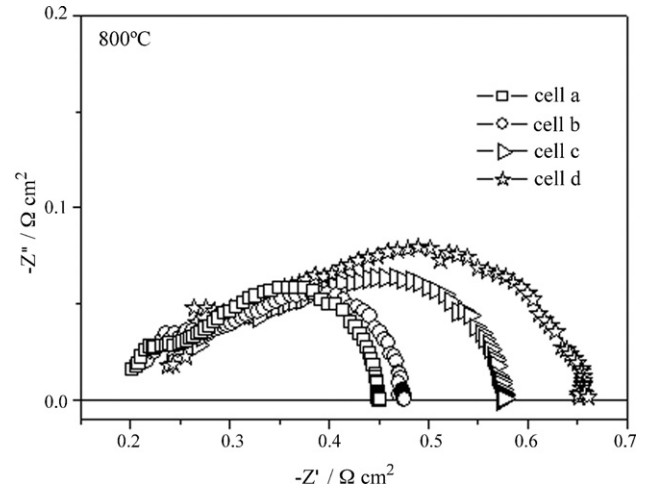

Fig. 3. Impedance spectra of symmetric cathode cell obtained at 800 °C in air.

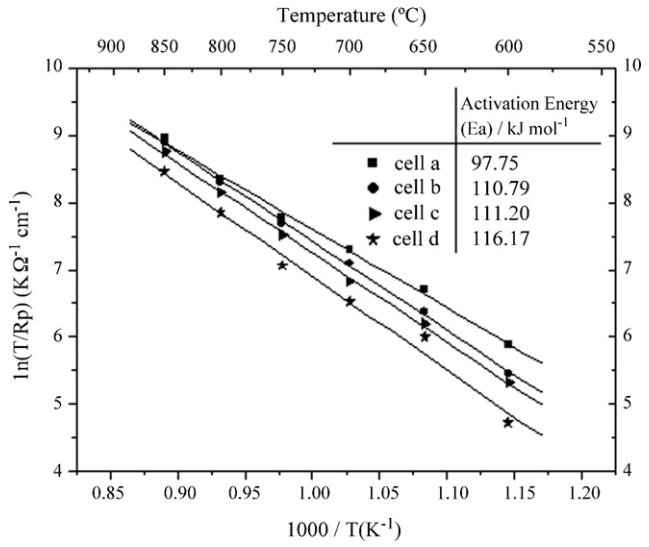

Fig. 4. Arrhenius plots of the interfacial polarization resistances for the cells a, b, c, and d.

a, b, and c, we can see that the interfacial polarization resistances decreased with an increase of the printing times of the LSCF-layer, under the condition of the same total printing time. For cell a, the LSM–YSZ and LSM–SDC layers act as "intermediators" between the YSZ electrolyte and the LSCF layers. According to the impedance data obtained from different testing temperatures, the temperature dependence of the interfacial polarization resistance for the four cells is given in Fig. 4, and the apparent activation energy (E_a) was also calculated from the slope of the $\ln(T/R_p)$ versus $1000/T$ plots. From Fig. 4, it can also be observed that cell "a" performs better.

3.3. Overpotential and impedance analysis measured using three-electrode method

According to the cathode components of cells "a" and "d", half-cells were fabricated and tested using the three-electrode method. Fig. 5 shows the cathodic polarization curves for the LSCF–LSM multi-layer composite cathode tested at 750 °C in air, compared with that of the conventional LSM/LSM–YSZ composite cathode. It can be clearly seen that there is a remarkable improvement in

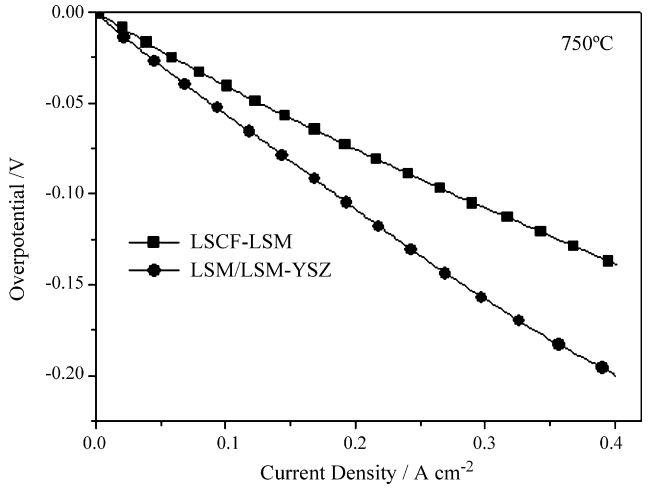

Fig. 5. Polarization curves for the LSCF–LSM multi-layer composite cathode and the LSM/LSM–YSZ composite cathode at 750 °C.

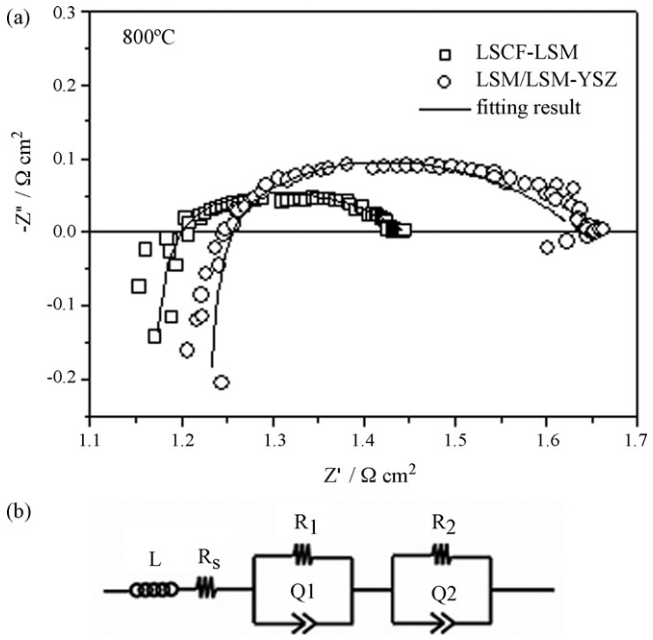

Fig. 6. (a) Impedance spectra of the LSCF–LSM multi-layer composite cathode and the LSM–YSZ composite cathode measured using the three-electrode method at 800 °C; (b) equivalent circuit.

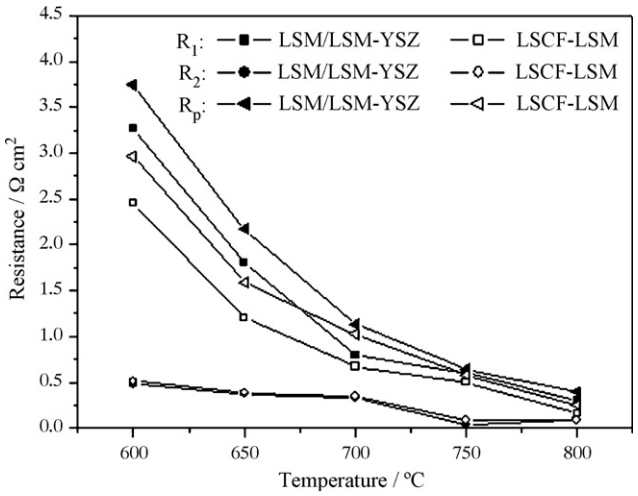

Fig. 7. Fitting results of R_1, R_2, and R_p as a function of temperature for the LSCF–LSM multi-layer composite cathode and the LSM–YSZ composite cathode.

electrode performance when the LSCF–LSM multi-layer cathode is used to replace the conventional one. At a current density of 0.4 A cm^{-2}, the LSCF–LSM multilayered cathode exhibits a cathodic overpotential lower than 0.13 V, while that of the LSM/LSM–YSZ cathode is about 0.20 V.

Fig. 6(a) shows the impedance spectra for the two cathodes measured using the three-electrode method under open-circuit-potential conditions. The equivalent circuit for fitting is also given in Fig. 6(b). The impedance spectra consisted of two arcs, indicating that there were at least two-electrode processes corresponding to the two arcs during molecular oxygen reduction. A high-frequency inductive component (L) coming from the measuring system is visible at high temperature; the series resistance, R_s, corresponds to the overall ohmic resistance from the electrolyte, electrodes and the connection wires; Q is the constant-phase element, and (R_1, Q_1) and (R_2, Q_2) correspond to the high- and low-frequency arcs, respectively [16]. The high-frequency arc (R_1, Q_1) corresponds to charge transfer of oxygen ions at the electrode/electrolyte interface [21–23]. The low-frequency arc (R_2, Q_2) reflects the oxygen adsorption or dissociation process [7]. The total interfacial polarization resistance (R_p) is the sum of R_1 and R_2. As expected, a smaller polarization resistance with a value of 0.25 Ω cm^2 at 800 °C is obtained for the LSCF–LSM multi-layer cathode, compared with that of 0.41 Ω cm^2 for the conventional LSM/LSM–YSZ composite cathode at the same temperature. Fig. 7 shows the fitting results of R_1, R_2 and R_p for the LSCF–LSM multi-layer composite cathode and the LSM/LSM–YSZ composite cathode. It is found that the resistance R_1, associated with the charge transfer of oxygen ions at the electrode/electrolyte interface, governs the total cathode resistance (R_p). For the LSCF–LSM multi-layer composite cathode, the decrease of total resistance is mainly the result of its reduction, suggesting that O_2 reduction on the porous LSCF–LSM multilayered electrode was limited primarily by the charge-transfer process, presumably occurring at the TPB [17]. These results elucidated that LSCF not only enhanced the electrical conductivity, but also improved the reaction rate of oxygen reduction at the interface between the cathode and electrolyte, because LSCF has higher electrical conductivity, surface oxygen exchange coefficients, and oxide-ion diffusivities [24,25].

Fig. 8 shows SEM micrographs of cross-sections of the LSCF–LSM and LSM/LSM–YSZ cathodes. It can be seen that the YSZ elec-

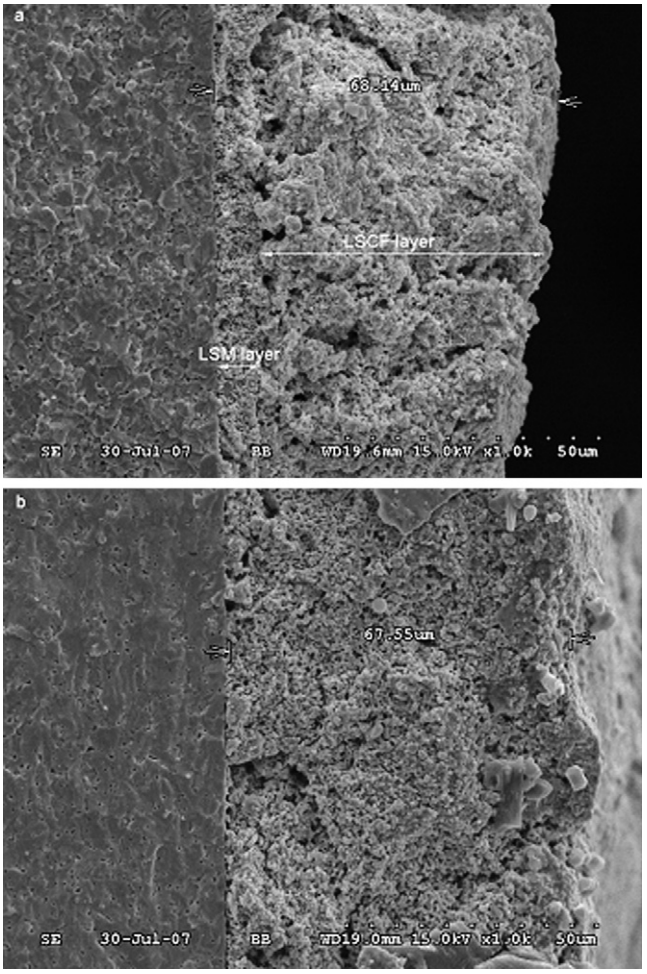

Fig. 8. SEM micrographs of cross-sections of the cathodes after electrochemical testing: (a) LSCF–LSM multi-layer composite cathode; (b) LSM/LSM–YSZ composite cathode.

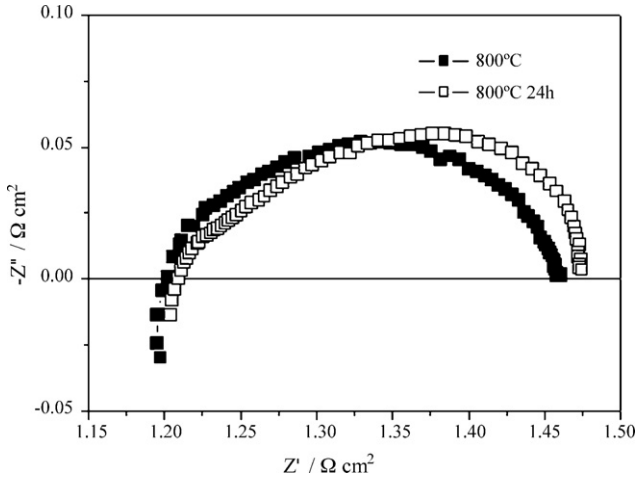

Fig. 9. Impedance spectra for the 24 h test of the LSCF–LSM multi-layer composite cathode.

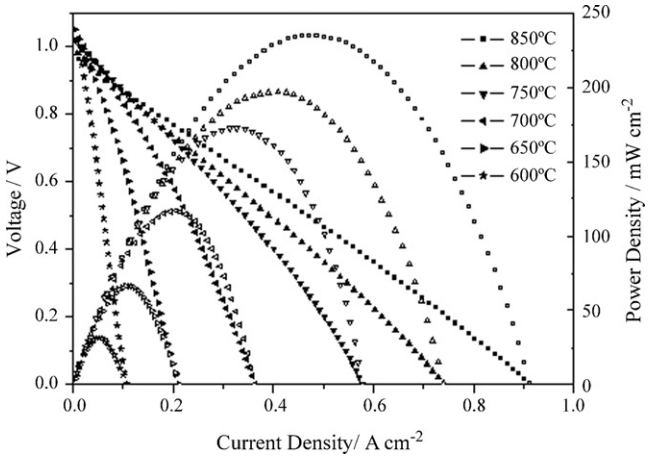

Fig. 10. Cell voltages (solid symbols) and power densities (open symbols) as a function of the current density of the YSZ-supported cell with LSCF–LSM multi-layer composite cathode, measured in humidified H_2 and air in the temperature range 600–850 °C.

trolytes are dense, while the cathodes are porous. The average thickness of both the electrodes is about 60–70 μm. Hart et al. [26] found the three-phase reaction zone could be extended after materials with higher ionic conductivity had been used, and they reported that better performance could be obtained when the thickness of cathodes was controlled at about 50 μm. Furthermore, Murray and Barnett [27] prepared an LSM–GDC (50:50 wt.%) composite cathode on GDC electrolyte and found the cathodic polarization was 0.34 Ω cm^2 at 750 °C, almost 24 times lower than that of the pure LSM cathode (8.19 Ω cm^2 at 750 °C under open-circuit conditions) on the YSZ electrolyte substrate. Zhu et al. [23] reported that an LSCF–SDC composite cathode showed a lower polarization resistance of 0.23 Ω cm^2 on an SDC electrolyte at 700 °C. All these workers supposed that the composite cathode improved the interfacial contact and expanded the TPB, which provided a guide to the improvement of the cathode electrochemical performance. So, it is evident that the LSM–SDC and LSCF–SDC middle layers in our multi-layer composite cathode play an important role in improving the cathode properties. They can reduce the mismatch of TEC between the LSM and LSCF layers, providing a better adhesion between them. Furthermore, and most importantly, they can extend the length of the TPB.

Fig. 9 shows the impedance spectra for the long-term testing of the LSCF–LSM multi-layer composite cathode. It was observed that there was only about 4% attenuation of the polarization resistance after the LSCF–LSM multi-layer composite cathode had been tested at 800 °C for 24 h, implying that it was mechanically stable.

3.4. Performance of single cells

We applied the LSCF–LSM multi-layer composite cathode to an YSZ electrolyte-supported SOFC. The curves of cell voltage and the corresponding power density versus current density are shown in Fig. 10. The cell shows encouraging performance, with maximum output power densities of 234, 196, and 173 mW cm^{-2} at 850, 800, and 750 °C, respectively. For comparison, a SOFC with the conventional LSM/LSM–YSZ cathode was also tested and its maximum power densities at the different temperatures are plotted in Fig. 11, together with the above results with LSCF–LSM cathode. With the same thickness of YSZ electrolyte, the advantage of the LSCF–LSM multi-layer cathode is obvious, with maximum SOFC power densities 30–40% higher than those with a conventional LSM/LSM–YSZ cathode.

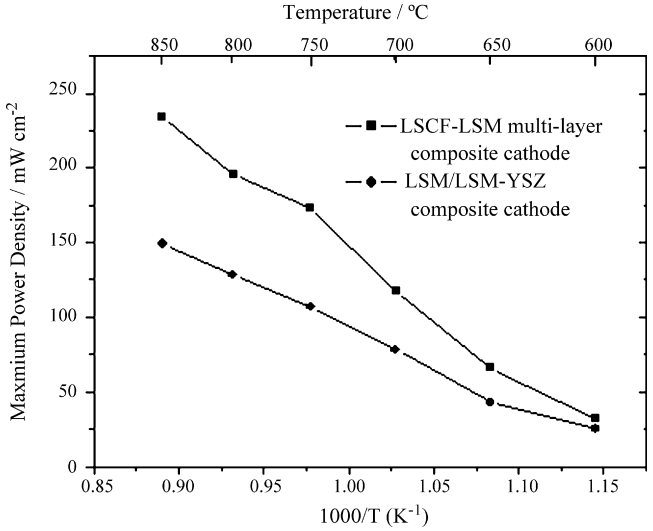

Fig. 11. Comparison of maximum power densities of YSZ-supported cells with the LSCF–LSM multi-layer composite cathode and the LSM/LSM–YSZ composite cathode.

4. Conclusions

An LSCF–LSM multi-layer composite cathode was prepared by the screen-printing technique on an YSZ substrate. It was investigated in comparison with a conventional LSM/LSM–YSZ cathode by means of cathodic polarization curves and electrochemical impedance spectroscopy. The LSCF–LSM multi-layer composite cathode shows better electrochemical performance than that of an LSM/LSM–YSZ composite cathode, with a cathodic polarization value of 0.25 Ω cm^2 at 800 °C, nearly 40% lower than that of an LSM/LSM–YSZ electrode. In addition, the maximum output power of an YSZ-electrolyte-supported SOFC using the LSCF–LSM multi-layer composite cathode is 30–40% higher than that with the traditional cathode. So, the experimental results suggest that the LSCF–LSM multi-layer composite cathode is a good choice for improving the performance of YSZ-electrolyte SOFCs.

Acknowledgements

The authors gratefully acknowledge financial support from the National Hi-tech 863 project of China (2007AA05Z136) and the Department of Science and Technology of Guangdong Province (2005B50101007) and the Department of Education of Guangdong Province (B15N9060210).

References

[1] S.P. Jiang, J. Power Sources 124 (2003) 390–402.
[2] M.J.L. Østergd, C. Clausen, C. Bagger, M. Mogensen, Electrochim. Acta 40 (1995) 1971–1981.
[3] S.P. Jiang, Solid State Ionics 146 (2002) 1–22.
[4] T. Tsai, S.A. Barnett, Solid State Ionics 93 (1997) 207–217.
[5] J.T. Brown, Energy 11 (1986) 209–229.
[6] I. Yasuda, K. Ogasawara, M. Hishinuma, T. Kawada, M. Dokiya, Solid State Ionics 86–88 (1996) 1197–1201.
[7] X.Y. Xu, C.R. Xia, G.L. Xiao, D.K. Peng, Solid State Ionics 176 (2005) 1513–1520.
[8] J.D. Zhang, Y. Ji, H.B. Gao, T.M. He, J. Liu, J. Alloy Compd. 395 (2005) 322–325.
[9] G.Ch. Kostogloudis, C. Ftikos, Solid State Ionics 126 (1999) 143–151.
[10] S. Carter, A. Selcuk, R.J. Chater, J. Kajda, J.A. Kilner, B.C.H. Steele, Solid State Ionics 53–56 (1992) 597–605.
[11] Y. Teraoka, T. Nobunaga, K. Okamoto, M. Miura, N. Yamazoe, Solid State Ionics 48 (1991) 207–212.
[12] C.C. Chen, M.M. Nasrallah, H.U. Anderson, in: S.C. Singhal, H. Iwahara (Eds.), SOFC-III, PV 93-4, Electrochemical Society, Pennington, NJ, 1993, p. 252.
[13] F. Tietz, V.A.C. Haanappel, A. Mai, J. Mertens, D. Stöver, J. Power Sources 156 (2006) 20–22.
[14] S.Y. Li, Z. Lü, B. Wei, X.Q. Huang, J.P. Miao, G. Cao, R.B. Zhu, W.H. Su, J. Alloy Compd. 426 (2006) 408–414.
[15] Y.H. Zhang, X.Q. Huang, Z. Lü, X.D. Ge, J.H. Xu, X.S. Xin, X.Q. Sha, W.H. Su, Solid State Ionics 177 (2006) 281–287.
[16] F. Qiang, K.N. Sun, N.Q. Zhang, X.D. Zhu, S.R. Le, D.R. Zhou, J. Power Sources 168 (2007) 338–345.
[17] S.B. Adler, Solid State Ionics 111 (1998) 125–134.
[18] A. Barbucci, M. Viviani, P. Carpanese, D. Vladikova, Z. Stoynov, Electrochim. Acta 51 (2006) 1641–1650.
[19] J. Liu, S.A. Barnett, Solid State Ionics 158 (2003) 11–16.
[20] J. Liu, Z. Lü, S.A. Barnett, Y. Ji, W.H. Su, 9th International Symposium on Solid Oxide Fuel Cells, Electrochemical Society Proceedings 07, 2005, p. 1976.
[21] Y.J. Leng, S.H. Chan, S.P. Jiang, K.A. Khor, Solid State Ionics 170 (2004) 9–15.
[22] F.S. Baumann, J. Fleig, M. Konuma, U. Starke, H.U. Habermeier, J. Maier, J. Electrochem. Soc. 152 (2005) A2074–A2079.
[23] X.D. Zhu, K.N. Sun, N.Q. Zhang, X.B. Chen, L.J. Wu, D.C. Jia, Electrochem. Commun. 9 (2007) 431–435.
[24] S. Kim, S. Wang, X. Chen, Y.L. Yang, N. Wu, A. Ignatiev, A.J. Jacobson, B. Abeles, J. Electrochem. Soc. 147 (2000) 2398–2406.
[25] A.V. Virkar, J. Chen, C.W. Tanner, J.W. Kim, Solid State Ionics 131 (2000) 189–198.
[26] N.T. Hart, N.P. Brandon, M.J. Day, N.R. Lapena, J. Power Sources 106 (2002) 42–50.
[27] E.P. Murray, S.A. Barnett, Solid State Ionics 143 (2001) 265–273.